

# The Dislocation Density of Acicular Ferrite in Steel Welds

*It is estimated that the dislocation density of acicular ferrite contributes 21 ksi to its strength*

BY J. R. YANG AND H. K. D. H. BHADSHIA

**ABSTRACT.** The dislocation density of acicular ferrite in a steel weld deposit has been estimated using transmission electron microscopy, at about  $10^{14} \text{ m}^{-2}$ , contributing approximately 145 MPa (21 ksi) to its strength.

## Introduction

Acicular ferrite is a phase formed by the transformation of austenite during cooling of low-alloy steel weld deposits (Ref. 1). It exhibits a thin-plate morphology and forms in a temperature range where reconstructive transformations become relatively sluggish and give way to displacive transformations. The transformation is found to exhibit an "incomplete-reaction phenomenon" in the sense that the formation of acicular ferrite ceases before the residual austenite reaches its equilibrium composition (Refs. 2, 3). The growth of acicular ferrite is known to be accompanied by an invariant-plane strain shape deformation (Ref. 3). Since the transformation occurs at fairly high temperatures where the yield strengths of the phases concerned are relatively low, the shape change may to some extent be plastically accommodated. This plastic deformation would in turn cause the dislocation density of the acicular ferrite and any residual austenite to increase. While it is known qualitatively that the dislocation density of acicular ferrite is fairly high (Refs. 4, 5), there are few quantitative data to this effect. A recent review (Ref. 6) quoted the dislocation density to be  $10^{12} - 10^{14} \text{ m}^{-2}$ , based on the work of Tuliani (Ref. 7) and Watson (Ref. 8), although the details of the measurements were not mentioned. The work presented here is part of a program of research on the quantitative pre-

diction of weld metal microstructure and properties. It deals specifically with the measurement of the dislocation density of acicular ferrite, with a view to estimating the contribution of dislocations to the strength of acicular ferrite.

## Experimental Techniques

The specimens studied were taken from the top layer of a manual metal arc weld of chemical composition: Fe-0.031C-0.40Si-1.68Mn-2.46Ni-0.17Mo wt-% (the weld also contained the following elements: 0.04Cr-0.01V-0.005S-0.008P-0.02Al-0.03Ti-0.01Nb-0.0333O-0.0080N wt-%). The chemical analysis was carried out using a spectroscopic technique, although the concentrations of oxygen and nitrogen were measured using *Leco* furnaces (Ro-17 and Tn-15), with 50 g of material for each determination to ensure representative results. The welds were made using 4-mm ( $5/32$ -in.) diameter electrodes (E10016-G type, as defined by the American Welding Society); the joint geometry was designed according to BS639 in order to avoid dilution from the base plate. Welding was carried out in the flat position, using the stringer bead technique; the base plate thickness was 20 mm (0.8 in.). The welding current and voltage used were 180 A and 23 V (DCEP), respectively (nominal arc energy  $\approx 2 \text{ kJ mm}^{-1}$ ); the weld consisted of some 21 passes with 3 passes per layer, deposited at a speed of

about  $0.002 \text{ m s}^{-1}$ . The interpass temperature was typically  $250^\circ\text{C}$  ( $482^\circ\text{F}$ ).

Transmission electron microscopy samples were prepared from 3-mm (0.12-in.) diameter disks machined from the top layer of the weld, containing the as-deposited, primary microstructure. The disks were mechanically ground down to a thickness of 0.08 mm (0.003 in.) on 1200-grit SiC paper. The specimens were then twin-jet electropolished using a 5% perchloric acid, 25% glycerol and 70% ethanol mixture at ambient temperature and 45 V. They were examined using a Philips EM400T transmission electron microscope operated at 120 kV.

## Results and Discussion

The dislocation structure observed in thin foil samples can be approximately representative of the bulk material if precautions are taken during the preparation of foils. It is unlikely that dislocations are introduced during thinning, but the subsequent handling of specimens can lead to accidental deformation. The dislocations introduced in this way tend to be long and nearly straight (Ref. 9) since they lie parallel to the foil surface. This damage is easily recognized with experience and can be avoided in ordinary polycrystalline specimens. In any event, great care was exercised during the handling of thin foil specimens. Other factors such as surface image forces may make the dislocation leave the foil, but the use of oxidizing polishing solutions usually leaves a thin oxide film on the surface of the foil and prevents any such losses.

Each dislocation density determination was based on measurements from ten micrographs, taken at magnifications of 60,000 to 100,000. These magnifications were chosen because they are high enough to resolve individual dislocations; at the same time, the magnifications are low enough to ensure that the micrographs had the same apparent dislocation content as the surrounding regions.

Ham (Ref. 10) and Hirsch, *et al.* (Ref. 11),

## KEY WORDS

Dislocation Density  
Acicular Ferrite  
Low-Alloy Steel Weld  
Strengthening Effect  
Burgers Vectors  
Ferrite Crystals  
Dislocation Structure  
TEM Examination

J. R. YANG is with the Graduate Institute of Materials Engineering, National Taiwan University, Taipei, Taiwan. H. K. D. H. BHADSHIA is with the Department of Materials Science and Metallurgy, University of Cambridge, Cambridge, England.

**Table 1—Extinction Distance  $\zeta_g$  (Å) in Ferrite for 100 and 120 kV Electron Accelerating Voltage**

Reflection g	Extinction Distance $\zeta_g$ (Å)	
	100 kV	120 kV
110	270	289
200	395	423
211	503	538
220	606	648
310	712	762

**Table 2—Proportion of Burgers Vectors Invisible in Body-Centered Cubic Metals under Different Two-Beam Diffraction Conditions**

Diffraction Condition	Pro- portion of a/2 <111>	Pro- portion of a <100>	Pro- portion of a <110>
	Burgers Vectors Invisible	Burgers Vectors Invisible	Burgers Vectors Invisible
g = <110>	0.5	0.33	0.17
g = <200>	0	0.67	0.33
g = <211>	0.25	0	0.17

showed that, provided the dislocations are randomly oriented, their densities measured in units of  $m/m^3$  are given by  $\rho = 2N M/Lt$ , where N is the number of intersections that a random straight test line laid on a transmission electron micrograph makes with the dislocations, L is the total length of the test line, t is the thickness of foil and M is the magnification of the micrograph. In order to minimize any dislocation orientation effects, the intersections were counted using a series of circles, instead of random straight lines (Ref. 12). Two concentric circles, 4.40 and 6.28 cm (1.7 and 2.5 in.) in circumference, respectively, were used.

Foil thickness was in each case estimated by counting extinction contours (Ref. 13). Provided that two-beam conditions are used during imaging, the foil thickness is given by  $t = \eta_g \zeta_g$ , where  $\eta_g$  is the number of extinction fringes observed at an inclined boundary, when the diffracted beam is represented by the reciprocal lattice vector g. The term  $\zeta_g$  is the extinction distance for that g vector and accelerating voltage. In addition, the foil should be oriented such that the grain examined is at the Bragg condition (Refs. 13, 14), the condition for which the extinction distance is defined (and is maximum). The extinction distances are listed in Table 1. They are from Ref. 16 and are corrected for the higher electron accelerating voltage used in the present experiments, by multiplying by a factor corresponding to the ratio of electron velocity at 120 kV to

that at 100 kV. It should be noted that the use of thickness fringes in this manner can in principle lead to some errors even though two-beam imaging conditions are used, depending on the diffraction conditions in the adjacent grain.

A series of micrographs was taken in bright field using two-beam conditions, the diffracted beam being 110, 200 or 112. The use of two-beam conditions must render some dislocations invisible, but the percentage of invisible dislocations can be estimated, subject to the following assumptions:

1) All dislocations have Burgers vectors of the type  $\underline{b} = a/2 <111>$ , where a is the lattice parameter of acicular ferrite, i.e., all the dislocations are undissociated. It is, however, possible that some dislocations have Burgers vectors of the type  $b = a <100>$  or  $b = a <110>$  (Ref. 17). The possible errors introduced by ignoring the presence of these Burgers vectors are discussed later.

2) The dislocations are randomly distributed both in space and amongst the four possible variants of the Burgers vector.

3) All dislocations satisfying the invisibility criterion ( $\underline{g} \cdot \underline{b} = 0$ ) are completely out of contrast.

In fact, the invisibility criterion  $\underline{g} \cdot \underline{b} = 0$  is applicable only to screw dislocations. For edge dislocations, both  $\underline{g} \cdot \underline{b}_e$  and  $\underline{g} \cdot \underline{b}_e \wedge \underline{u}$  (where  $\underline{b}_e$  and  $\underline{u}$  represent the Burgers vector and line vector, respectively, of an edge dislocation) must be zero for complete invisibility. However, in practice, only faint residual contrast occurs for edge dislocations where  $\underline{g} \cdot \underline{b}_e = 0$ , but  $\underline{g} \cdot \underline{b}_e \wedge \underline{u} \neq 0$  and this has been interpreted as indicating dislocation invisibility (Ref. 16).

The values of  $\underline{g} \cdot \underline{b}$  for the first three reflections and the  $a/2 <111>$  Burgers vectors in body-centered cubic metals are listed in Table 2. The proportion of the  $a/2 <111>$  Burgers vectors invisible under different two-beam diffraction conditions are summarized in Table 3. A typical electron micrograph used in the estimation of dislocation density is illustrated in Fig. 1, which also displays five extinction fringes on the upper grain boundary, used for estimating the foil thickness at 269 nm. The average foil thickness for the measurements is of the order of  $245 \pm 44$  nm. After the dislocation density had been measured directly from an electron micrograph, it was corrected by adding the part, which should be invisible due to the two-beam imaging method, assuming that most of the dislocations have the Burgers vector  $a/2 <111>$ . However, Dingley and Hale have suggested that up to about 40% of the dislocations might in fact have the Burgers vectors  $a <100>$  and  $a <110>$  in equal proportion (Ref. 17). Using this information and the data given in Table 2, the assumption that all the dis-

locations have  $\underline{b} = a/2 <111>$  could lead to errors that are estimated to be as follows:

1) For  $g = <110>$  the dislocation density could be overestimated by about 26%.

2) For  $g = <200>$  the dislocation density could be underestimated by about 20%.

3) For  $g = <211>$  the dislocation density could be overestimated by 7%.

A complete list of experimental data is presented in Table 4. The average corrected dislocation density of acicular ferrite is of the order of  $(3.90 \pm 1.97) \times 10^{14} m^{-2}$ . The variations in density are larger than the errors discussed above.

The primary microstructure of a low-alloy steel weld consists of a mixture of allotriomorphic ferrite ( $\alpha$ ), Widmanstätten ferrite ( $\alpha_w$ ) and acicular ferrite ( $\alpha_a$ ); the latter also contains "microphases," which are regions of martensite, retained austenite or pearlite. The yield strength ( $\sigma_p$ ) of such a microstructure can be factorized as follows (Refs. 18, 19):

$$\sigma_p = \sigma_{Fe} + \sum_i \sigma_{SS_i} + \sigma_\alpha V_\alpha + \sigma_a V_a + \sigma_w V_w$$

where  $\sigma_{Fe}$  is the intrinsic strength of pure annealed iron and the second term on the right represents solid solution strengthening contributions.  $\sigma_\alpha$ ,  $\sigma_w$  and  $\sigma_a$  represent the microstructural strengthening due to allotriomorphic ferrite, Widmanstätten ferrite, and acicular ferrite, respectively, and V represents the volume fraction of

**Table 3—The Values of  $\underline{g} \cdot \underline{b}$  for the First Three Reflections and the  $a/2 <111>$  Burgers Vector**

Reflection	Possible Burgers Vector			
	a/2 [111]	a/2 [111]	a/2 [111]	a/2 [111]
110	1	0	0	1
101	1	0	1	0
001	1	1	0	0
110	0	1	1	0
101	0	1	0	1
011	0	0	1	1
200	1	1	1	1
020	1	1	1	1
002	1	1	1	1
200	1	1	1	1
020	1	1	1	1
002	1	1	1	1
112	2	1	1	0
121	2	1	0	1
211	2	0	1	1
112	1	2	0	1
121	1	2	1	0
211	0	2	1	1
112	1	0	2	1
121	0	2	1	1
211	1	1	2	0
112	0	1	1	2
121	1	0	1	2
211	1	1	0	2

the phase concerned.

The microstructural strengthening term includes effects such as grain boundary and dislocation strengthening. The microstructural strengthening coefficient  $\sigma_a$  of acicular ferrite has been found to be  $402 \pm 29$  MPa, for a very large number of weld deposits (Ref. 18). This work allows the contribution due to the dislocation strengthening of acicular ferrite (i.e.,  $\sigma_D$ ) to be estimated as follows (Ref. 20):

$$\sigma_D = 0.38Gb\rho^{0.5}$$

where G is the shear modulus of the ferrite, b is the magnitude of the Burgers vector of the dislocations concerned and  $\rho$  is the dislocation density. Using this equation and the mean observed dislocation density,  $\sigma_D$  is estimated to be 145 MPa.

### Summary and Conclusions

The dislocation density of acicular ferrite has been estimated to be about  $10^{14} \text{ m}^{-2}$ , contributing approximately 145 MPa to the strength of acicular ferrite. These results will be of use in further detailed studies of the strength of acicular ferrite.

#### References

1. Bhadeshia, H. K. D. H. 1989. Bainite in steels. *Phase Transformations 87*, ed. G. W. Lorimer, Institute of Metals, London, England, pp. 309-314.
2. Yang, J. R., and Bhadeshia, H. K. D. H. 1987. Thermodynamics of the acicular ferrite transformation in alloy-steel weld deposits. *Advances in Welding Science and Technology*, ed. S. A. David, ASM, Materials Park, Ohio, pp. 187-191.
3. Strangwood, M., and Bhadeshia, H. K. D. H. 1987. The mechanism of acicular ferrite formation in steel weld deposits. *Advances in Welding Science and Technology*, ed. S. A. David, ASM, Materials Park, Ohio, pp. 209-213.
4. Kikuta, Y. 1983. Classification of microstructures in low-C, low-alloy steel weld metal and terminology. Committee of Welding Metallurgy of the Japan Welding Society, Report No. IX-1281-83, p. 15.
5. Harrison, P. L., Watson, M. N., and Farrar, R. A. 1981. How niobium influences SA mild steel weld metals. *Welding and Metal Fabrication*, pp. 161-169.
6. Farrar, R. A., and Harrison, P. L. Review: acicular ferrite in carbon-manganese weld metals. *J. Mat. Sci.* 22:3812-3820.
7. Tuliani, S. S. 1973. Ph.D. thesis, University of Southampton.
8. Watson, M. N. 1980. Ph.D. thesis, University of Southampton.
9. Hirsch, P., Howie, A., Nicholson, R. B., Pashley, D. W., and Whelan, M. J. 1977. *Electron Microscopy of Thin Crystals*. Published by Krieger, New York, N.Y.
10. Ham, R. K. 1961. The determination of dislocation densities in thin foils. *Phil. Mag.* 6:1183-1184.
11. Hirsch, P., Howie, P., Nicholson, R. B., Pashley, D. W., and Whelan, M. J. 1977. *Electron Microscopy of Thin Crystals*. Published by

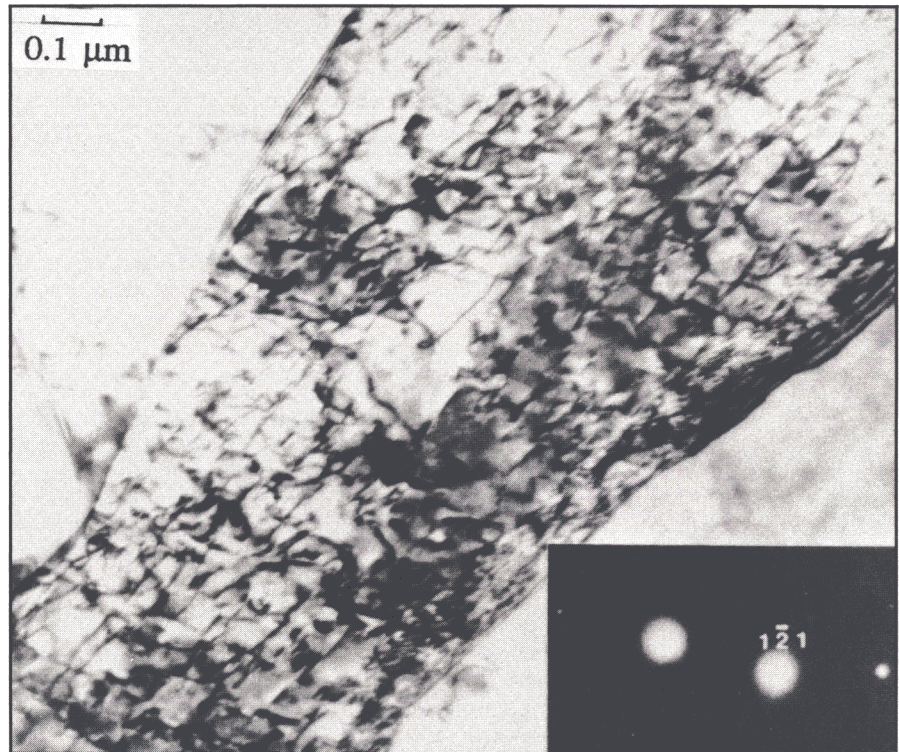


Fig. 1—Transmission electron micrograph showing a bright field image of a plate of acicular ferrite, taken using approximately two-beam imaging conditions.

Table 4—Experimental Data for the Calculation of Dislocation Density

Two-beam Condition g	No. of Extinction Fringes $\eta_g$	Thickness of Thin Foil t (Å)	Measured Dislocation Density ( $\text{m}^{-2}$ )	Corrected Dislocation Density ( $\text{m}^{-2}$ )
<112>	5	2690	$1.87 \times 10^{14}$	$2.49 \times 10^{14}$
<110>	5	1445	$4.90 \times 10^{14}$	$8.90 \times 10^{14}$
<112>	5	2690	$2.05 \times 10^{14}$	$2.73 \times 10^{14}$
<200>	6	2538	$2.47 \times 10^{14}$	$2.47 \times 10^{14}$
<112>	5	2690	$2.60 \times 10^{14}$	$3.46 \times 10^{14}$
<112>	5	2690	$2.53 \times 10^{14}$	$3.37 \times 10^{14}$
<110>	6	1734	$3.16 \times 10^{14}$	$6.32 \times 10^{14}$
<112>	5	2690	$2.18 \times 10^{14}$	$2.91 \times 10^{14}$
<112>	5	2690	$2.29 \times 10^{14}$	$3.05 \times 10^{14}$
<112>	5	2690	$2.46 \times 10^{14}$	$3.28 \times 10^{14}$

Krieger, New York, N.Y., p. 422.

12. Staker, M. R., and Holt, D. L. Dislocation cell size in deformed copper. *Acta Metall.* 20:569-579.

13. Hirsch, P., Howie, A., Nicholson, R. B., Pashley, D. W., and Whelan, M. J. 1977. *Electron Microscopy of Thin Crystals*. Published by Krieger, New York, N.Y., p. 416.

14. Murr, L. E. 1970. *Electron Optical Applications in Materials Science*. McGraw-Hill, p. 320.

15. Hirsch, P., Howie, A., Nicholson, R. B., Pashley, D. W., and Whelan, M. J. 1977. *Electron Microscopy of Thin Crystals*. Published by Krieger, New York, N.Y., p. 510.

16. Edington, J. W. 1975. *Practical Electron Microscopy in Materials Science*. MacMillan, London, 1975, p. 119.

17. Dingley, D. J., and Hale, K. F. 1966. Burgers vectors of dislocations in deformed iron and iron alloys. *Proceedings of the Royal Society (London)*, 295A pp. 55-71.

18. Sugden, A. A. B., and Bhadeshia, H. K. D. H. A model for the prediction of strength in steel weld deposits. *Metallurgical Transactions A*, 19A pp. 1597-1602.

19. Svensson, L. E., Gretoft, B., Sugden, A., and Bhadeshia, H. K. D. H. 1988. Computer-aided design of electrodes for arc welding processes: Part II, 2nd Int. Conf. Computer Technology in Welding, Welding Institute, Paper 24.

20. Keh, A. S., and Weissmann, S. Deformation structures in body-centered cubic metals. *Electron Microscopy and the Strength of Crystals*, G. Thomas and J. Washburn eds., Interscience, New York, N.Y. pp. 231-300.